Endocytic Recycling Compartments Altered in Cisplatin-Resistant Cancer Cells

Xing-Jie Liang,[1] Sushmita Mukherjee,[2] Ding-Wu Shen,[1] Frederick R. Maxfield,[2] and Michael M. Gottesman[1]

[1]Laboratory of Cell Biology, National Cancer Institute, NIH, Bethesda, Maryland and [2]Department of Biochemistry, Weill Medical College of Cornell University, New York, New York

Abstract

The clinical utility of cisplatin to treat human malignancies is often limited by the development of drug resistance. We have previously shown that cisplatin-resistant human KB adenocarcinoma cells that are cross-resistant to methotrexate and heavy metals have altered endocytic recycling. In this work, we tracked lipids in the endocytic recycling compartment (ERC) and found that the distribution of the ERC is altered in KB-CP.5 cells compared with parental KB-3-1 cells. A tightly clustered ERC is located near the nucleus in parental KB-3-1 cells but it appears loosely arranged and widely dispersed throughout the cytoplasm in KB-CP.5 cells. The altered distribution of the ERC in KB-CP.5 cells is related to the amount and distribution of stable detyrosinated microtubules (Glu-α-tubulin), as previously shown in Chinese hamster ovary B104-5 cells that carry a temperature-sensitive Glu-α-tubulin allele. In addition, B104-5 cells with a dispersed ERC under nonpermissive conditions were more resistant to cisplatin compared with B104-5 cells with a clustered ERC under permissive conditions. We conclude that resistance to cisplatin might be due, in part, to reduced uptake of cisplatin resulting from an endocytic defect reflecting defective formation of the ERC, possibly related to a shift in the relative amounts and distributions of stable microtubules. (Cancer Res 2006; 66(4): 2346-53)

Introduction

Cisplatin is widely used in the treatment of solid tumors (1). The mechanism of cisplatin entry into the cell and its intracellular transport from the cytosol to the nucleus are complex. Recent studies suggest that entry requires interaction with membrane proteins (2) and that endocytic recycling is defective in cisplatin-resistant cells (3). After entry, cisplatin becomes aquated and ~1% of the total cellular cisplatin can then interact with macromolecules like DNA to form intrastrand or interstrand adducts (4). The aquated platinum species binds preferentially to the highly nucleophilic N-7 positions of guanine and adenine (5). Apart from DNA and RNA, cisplatin also interacts with intracellular proteins and polypeptides (6) and with negatively charged phospholipids in intact human erythrocytes and tumor cells (7–9). Despite the obvious interactions of cisplatin with membrane components, few studies have been done on entry of cisplatin into target cells and its facilitated transport (10, 11). Because many cisplatin-resistant cells show decreased uptake of cisplatin, the identification of specific transport pathways responsible for drug resistance should provide targets for therapy aimed at circumventing or decreasing cisplatin resistance.

We have previously shown that cisplatin-resistant human KB adenocarcinoma cells have altered endocytic recycling, shown by the mislocalization of membrane proteins (12). To study the recycling pathway, the transferrin receptor and its ligand, transferrin, have been extensively used (13). Within early endosomes, Fe^{3+} dissociates from transferrin and the transferrin receptor-transferrin complexes either return directly to the plasma membrane or reach a network of tubular membranes, called the endocytic recycling compartment (ERC), before returning to the plasma membrane. Transferrin is a bona fide marker of the ERC and, at steady state, a majority of the internalized transferrin localizes to this compartment (14). The ERC is concentrated in the perinuclear region of many cell types and most membrane components pass through it along their endocytic recycling itineraries. Some evidence indicates that the ERC has sorting abilities of its own and is involved in the delivery of membrane proteins to the *trans*-Golgi network (13). The ERC has been confirmed to be involved in receptor and lipid recycling (13, 15) and is characterized by its tubulovesicular morphology and dependence on intact microtubules for localization (16).

In this study, we use fluorescently labeled transferrin, as well as fluorescent lipid analogues, to show an abnormal morphology of the ERC in cisplatin-resistant cells. Instead of being concentrated in the perinuclear area, as in the parental cells, the ERC tubules in cisplatin-resistant cells are distributed throughout the cytoplasm. Our results further show that this altered distribution of the ERC is similar to that seen with increased stable, detyrosinated microtubules (Glu-α-tubulin). Interestingly, mutant Chinese hamster ovary (CHO) B104-5 cells with this microtubule defect are cisplatin resistant under nonpermissive conditions compared with mutant cells under permissive conditions or to parental CHO TRVb-1 cells under conditions nonpermissive for the mutant. These ERC tubules with abnormal distribution in cisplatin-resistant cells also show an altered intraorganellar pH, as well as a change in the rate of metabolism of a lipid species (i.e., sphingomyelin). Furthermore, fluorescently labeled methotrexate and cisplatin colocalize with the ERC structure labeled by transferrin. We conclude that cisplatin resistance and cross-resistance to methotrexate in our cisplatin-resistant cells may be due to a defect in the formation and distribution of the ERC.

Note: X-J. Liang and S. Mukherjee contributed equally to this work.

X-J. Liang is currently at Surgical and Molecular Neuro-oncology Unit, Surgical Neurology Branch, National Institute of Neurological Disorders and Stroke, NIH, Bethesda, MD 20892.

Requests for reprints: Michael M. Gottesman, Laboratory of Cell Biology, National Cancer Institute, NIH, Room 2108, Building 37, 37 Convent Drive, Bethesda, MD. Phone: 301-496-1530; Fax: 301-402-0450; E-mail: mgottesman@nih.gov.

©2006 American Association for Cancer Research.

doi:10.1158/0008-5472.CAN-05-3436

Downloaded from cancerres.aacrjournals.org on May 15, 2021. © 2006 American Association for Cancer Research.

Materials and Methods

Cell lines and culture conditions. KB-3-1 was originally derived from human KB epidermoid carcinoma cells (a variant of HeLa) after two subclonings from the parental cells (17). The cisplatin-resistant KB-CP.5 cells were selected for resistance to 0.5 μg/mL cisplatin in a single step and they were maintained in medium containing 0.5 μg/mL cisplatin for these experiments (12). B104-5 cells, a temperature-sensitive mutant CHO cell line, were isolated from parent TRVb-1 cells that lack the endogenous transferrin receptor and stably express the human transferrin receptor. B104-5 cells, unlike the parental TRVb-1 cells, do not grow well at the nonpermissive temperature of 39°C. They are normally grown in Ham's F12 medium containing bicarbonate, 5% fetal bovine serum, 2% penicillin-streptomycin, and 200 μg/mL G418 (Geneticin) at the permissive temperature of 32°C. The mutant TRVb-1 cell line (B104-5) is frequently used to study the function of Glu-α-tubulin (18).

Endocytic compartments labeled with various markers. The KB-3-1 and KB-CP.5 cells were labeled for 1 minute at 37°C with NBD-sphingomyelin, $DiIC_{16}$, $DiIC_{12}$, or Alexa 488-transferrin, rinsed, and chased for 30 minutes at 37°C. All lipid analogues (NBD-sphingomyelin, $DiIC_{16}$, and $DiIC_{12}$) were added from stocks previously loaded on fatty acid–free bovine serum albumin (BSA) to ensure efficient transfer of monomers to the plasma membrane (19). Cells labeled with $DiIC_{16}$, $DiIC_{12}$, or Alexa 488-transferrin were imaged live using wide-field microscopy. Cells labeled with NBD-sphingomyelin were chilled by washing with ice-cold medium (~0°C) and held on ice for 10 minutes for equilibration. Then, the NBD-sphingomyelin on the plasma membrane was extracted by incubating the cells on ice with medium containing 5% w/v fatty acid–free BSA, a method known as "back exchange." This was done four times, 10 minutes each for a total of 40 minutes (20, 21). NBD-sphingomyelin–labeled cells were then fixed with 3% paraformaldehyde for 15 minutes at room temperature and imaged using wide-field microscopy.

NBD-sphingomyelin to NBD-ceramide conversion assay. Parental KB-3-1 and the cisplatin-resistant KB-CP.5 cells were grown in six-well tissue culture plates. Three wells were pooled for each sample. Cells were labeled with NBD-sphingomyelin, chased, and excess plasma membrane NBD-sphingomyelin was back exchanged as described in the previous section. After back exchange, cells were washed again with chilled medium and the total cell lipids were extracted with two changes of hexane/isopropanol (3:2, v/v) for 30 minutes each.

Lipids were dried under Argon and further dried by overnight storage under vacuum. The NBD-sphingomyelin and any converted NBD-ceramide were separated by TLC using a previously reported solvent system (chloroform/methanol/water/ammonium hydroxide at 72:48:9:2, v/v/v/v; ref. 22). Because the NBD-ceramide ran very close to the solvent front, the plates were first pre-run in pure chloroform to remove hydrophobic impurities. After the pre-run, the TLC plates were air-dried and the samples spotted in 20-μL chloroform each. NBD-sphingomyelin and NBD-ceramide standards were run on each plate to ascertain the position of the spots in the cell extracts.

After the TLC run, the plates were dried and the spots quantified using a Molecular Dynamics (Sunnyvale, CA) densitometer. The intensities of the spots were quantified using MetaMorph (Molecular Devices, Downingtown, PA) image analysis software. The images from the densitometric scans were first background corrected, and then integrated intensity was measured in a defined area covering the whole spot or a larger area (the same size area was chosen to measure all spots and its size was chosen so as to completely include the largest spot). All further calculations were done using the Microsoft Excel program.

Immunoblotting detection of Glu-α-tubulin and Tyr-α-tubulin. Cells were grown in 75-cm^2 cell culture flasks until 80% confluence and washed thrice with ice-cold PBS buffer. Using a rubber policeman, cells were scraped into 1 mL of radioimmunoprecipitation assay lysis buffer (1% NP40, 0.5% sodium deoxycholate, 0.1% SDS, 0.004% sodium azide in TBS) and passed 30 times through a ball-bearing homogenizer. The cellular fractions were separated as previously described (12). The samples were separated on a 4% to 20% Tris-Gly gradient gel and transferred onto nitrocellulose membranes. Subsequently, membranes were subjected to immunostaining with antibodies against Glu-α-tubulin, diluted 1:1,000, for 1 hour at room temperature (Chemicon, Inc., Temecula, CA) and against Tyr-α-tubulin under the same conditions (Novus Biologicals, Littleton, CO). Enhanced chemiluminescence reagents were used for developing signals as described by the manufacturer (Pierce Biotechnology, Rockford, IL).

Distribution of Glu-α-tubulin and Tyr-α-tubulin detected by immunohistochemistry. B104-5 cells were incubated at 32°C or 39°C individually for 3 days before fixation. The cells (KB-3-1, KB-CP.5, and B104-5 at 32°C or 39°C) were cultured on 18-mm glass coverslips, fixed in 3.3% paraformaldehyde freshly diluted in PBS for 15 minutes, and then permeabilized with 70% ethanol in PBS at −20°C for 10 minutes. Cells were subsequently washed with PBS and preblocked in 3% bovine serum albumin in PBS for 30 minutes, then incubated for 1 hour with a primary antibody against Glu-α-tubulin (Chemicon) and Tyr-α-tubulin (rat monoclonal YL1/2, Novus Biologicals), which was followed by 1-hour incubation with a rhodamine-conjugated secondary antibody (1:50; Jackson ImmunoResearch Laboratories, Inc., West Grove, PA) before being mounted on slides with fluorescence mounting medium. Controls with nonimmune immunoglobulin G (IgG) were negative. Cells were processed at room temperature and photographed by immunofluorescence under a laser scanning confocal microscope (MRC-1024 confocal scan head; Bio-Rad, Hercules, CA) at ×600 magnification. Background fluorescence was determined by applying only the second antibody, a rhodamine-conjugated AffiniPure goat anti-rat IgG.

***In vitro* colony formation assay.** Briefly, an *in vitro* colony-forming assay was used to obtain IC_{50} values for B104-5 and TRVb-1 cells to cisplatin. B104-5 and TRVb-1 cells were seeded at 400 cells per 60-mm dish at 32°C or 39°C. At the time of seeding, different concentrations of individual drugs (0.05-5 μg/mL) were added to the dishes. The medium with different concentrations of drugs was changed every week. After incubation for ~4 weeks, the colonies formed at each concentration of drug were stained with 0.5% methylene blue in 50% methanol and counted. The IC_{50} for each cell line was calculated based on the drug concentration that reduced the number of colonies to 50% of those in the control, drug-free medium. The values are means of triplicate determinations.

Results

Trafficking of lipid analogues to late endosomes/lysosomes is normal in cisplatin-resistant KB-CP.5 cells. It has been previously reported that cisplatin-resistant cells exhibit an alteration in endocytosis (23), and more specifically, that their lysosomes exhibit an elevated pH. We thus wanted to determine whether this alteration affects lipid trafficking into late endosomes/lysosomes. Toward this purpose, we labeled both parental KB-3-1 cells and the cisplatin-resistant KB-CP.5 cells with $DiIC_{16}$, which is a lipid analogue containing long saturated alkyl chains. We have previously shown that this lipid analogue is efficiently trafficked to late endosomes/lysosomes in CHO cells (19). As shown in Fig. 1*A*, after a half hour of chase, cell-associated $DiIC_{16}$ is observed on the plasma membranes and in dispersed punctate structures throughout the cells. These punctate structures are late endosomes/lysosomes because they also contain internalized high molecular weight dextrans.[3] Furthermore, there is no significant difference in the distribution patterns between the parental KB-3-1 and the cisplatin-resistant KB-CP.5 cells, indicating that at least bulk membrane trafficking from the plasma membranes to late endosomes/lysosomes is not severely affected in cisplatin-resistant cells.

[3] Unpublished data.

Downloaded from cancerres.aacrjournals.org on May 15, 2021. © 2006 American Association for Cancer Research.

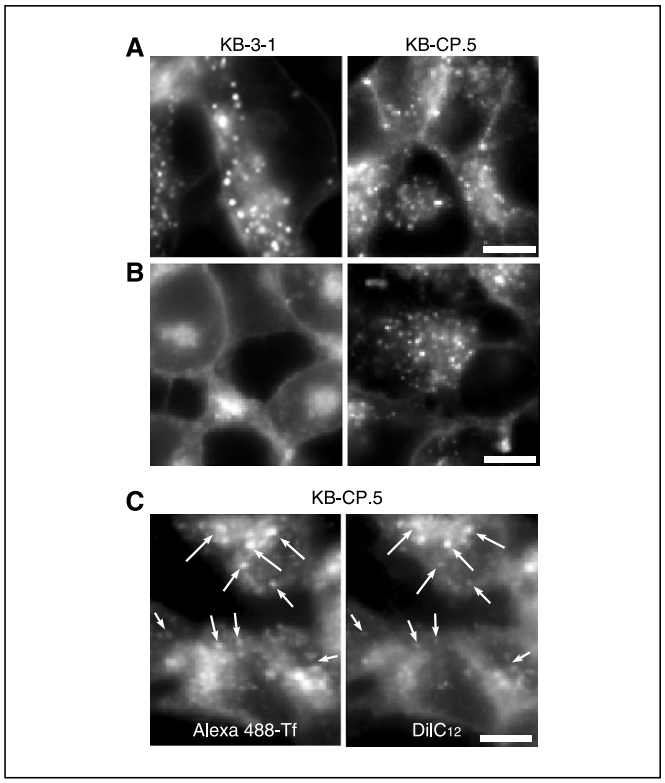

Figure 1. Altered ERC structures in cisplatin-resistant cells as shown by labeling with lipid probes. *A,* $DiIC_{16}$ labeling of KB-3-1 cells and KB-CP.5 cells. The cells were labeled for 1 minute at 37°C with $DiIC_{16}$ loaded on fatty acid–free BSA, rinsed, and chased for 30 minutes at 37°C. Cells were imaged live using wide-field microscopy. Bar, 10 μm. *B,* $DiIC_{12}$ labeling of KB-3-1 cells and KB-CP.5 cells. $DiIC_{12}$ labeling is similar to that of $DiIC_{16}$ mentioned above. Bar, 10 μm. *C,* colocalization of Alexa 488-transferrin and $DiIC_{12}$ in KB-CP.5 cells. The cells were labeled for 5 minutes at 37°C with 10 μg/mL Alexa 488-transferrin, rinsed, labeled for 1 minute with $DiIC_{12}$, loaded on fatty acid–free BSA, rinsed, and chased for 30 minutes at 37°C. Cells were imaged live using wide-field microscopy. *Arrows,* individual endosomes or clusters of endosomes, which are colocalized. Bar, 10 μm.

Lipid analogues that are normally trafficked to the ERC show altered distribution in cisplatin-resistant KB-CP.5 cells. Because our results, presented in Fig. 1*A*, suggested that trafficking from the plasma membrane to the late endosomes/lysosomes was relatively unaffected in cisplatin-resistant cells, we then decided to investigate the fate of lipid analogues that normally traffic via the other arm of endocytosis (i.e., lipid analogues that are recycled to the cell surface via the ERC). For this, we carried out experiments identical to those presented in Fig. 1*A*, except that the lipid analogue used was $DiIC_{12}$, an analogue containing a short alkyl chain that has been previously shown to recycle efficiently via the ERC in CHO cells (19). The results presented in Fig. 1*B* show that unlike $DiIC_{16}$, $DiIC_{12}$ exhibits a very different distribution in the cisplatin-sensitive versus cisplatin-resistant KB cells. In the normal parental (cisplatin-sensitive) KB-3-1 cells, the ERC distribution is similar to that of CHO cells. The ERC tubules are collected at the center of the cells near the microtubule organizing center and appear as a bright patch of fluorescence at the cell center (Fig. 1*B*). In contrast, in KB-CP.5 cells, the intracellular $DiIC_{12}$ appears as discrete punctate structures that are more peripherally distributed through the cells (Fig. 1*B*).

To further explain our observations, we double labeled KB-CP.5 cells with $DiIC_{12}$ and the green fluorescent Alexa 488-transferrin. Transferrin is a bona fide marker of the endocytic recycling pathway and its primary intracellular localization at steady state is in the ERC. Figure 1*C* shows that in KB-CP.5 cells, the transferrin distribution is punctate as well and the spots containing $DiIC_{12}$ and transferrin colocalize rather well in these cells (see Fig. 1*C*). This suggests that in KB-CP.5 cells, $DiIC_{12}$ is still trafficked to the ERC, just like the parental cells, but the morphology and distribution of this organelle are altered in these cells.

The structurally altered ERC in KB-CP.5 cells sequesters fluorescently labeled cisplatin. As shown in Fig. 1*B* and *C*, the ERC tubules in the KB-CP cells no longer accumulate at the cell center but instead are now dispersed throughout the cells. A similar distribution was previously observed for fluorescently labeled MRP1 and cisplatin (12, 24). We next asked whether such a change in ERC distribution had a functional consequence for cisplatin resistance. Toward this end, we double labeled KB-CP cells with fluorescently labeled transferrin and cisplatin to test where they would localize inside the cells. Interestingly, we found that the intracellular cisplatin accumulated inside these dispersed ERC tubules, which also contained transferrin (see Fig. 2). This observation suggests that there is something about the properties of these altered ERC tubules that sequester cisplatin, possibly restricting its delivery to other intracellular and nuclear targets,

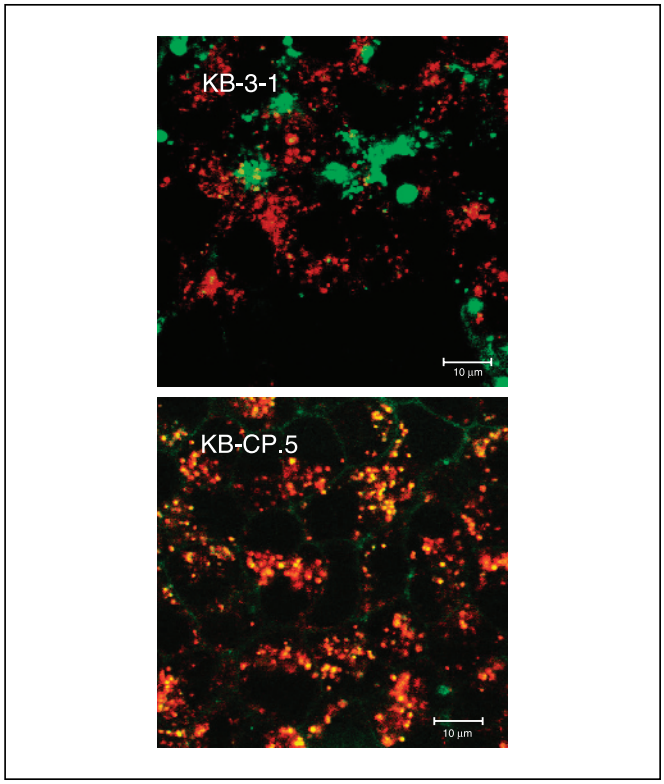

Figure 2. Indirect fluorescence to localize transferrin with fluorescently labeled cisplatin. Cells were labeled with Texas red-transferrin (*red*) and Alexa 488-cisplatin (*green*) as described in Materials and Methods. Labeled cells were excited at 488 and 568 nm, provided by a krypton laser as indicated, and fluorescence emissions at 520 and 598 nm were used for collecting green and red fluorescence, respectively, whereas differential interference contrast microscopy images of the same cells were collected in the third channel using a transmitted light detector. After sequential excitation, red and green fluorescent images of the same cells were merged for colocalization analysis. Colocalization of Texas red-transferrin (*red*) and Alexa 488-cisplatin (*green*) is shown in yellow.

Downloaded from cancerres.aacrjournals.org on May 15, 2021. © 2006 American Association for Cancer Research.

thereby reducing cell killing and making the cells resistant to cisplatin. We have since made the observation that these transferrin-containing ERC tubules also sequester fluorescently labeled methotrexate, another chemotherapeutic agent to which these cells are cross-resistant.

The structurally altered ERC in KB-CP.5 cells exhibits rapid sphingomyelin metabolism. To test whether the altered distribution observed with the normal recycling endocytic markers (i.e., $DiIC_{12}$ and transferrin) extended to other lipid analogues that normally recycle as well, we chose C6-NBD-sphingomyelin (NBD-sphingomyelin) as another model lipid. NBD-sphingomyelin has one short (six-carbon) acyl chain, which is conjugated at the terminal position with the fluorescent label, NBD. We and others have previously shown that this lipid analogue recycles efficiently in CHO cells (20, 21). Indeed, this is what was observed when the parental KB cells were labeled with NBD-sphingomyelin and chased for a half hour to reach steady state (Fig. 3*A*). These cells show only the intracellular NBD-sphingomyelin because the NBD-sphingomyelin on the cell surface, which normally interferes with the observation of intracellular distribution, has been back exchanged using excess fatty acid–free BSA, using established procedures (20, 21).

However, when the same experiment was carried out in the KB-CP.5 cells, we found that the distribution of the NBD fluorescence in these cells was rather unusual, and although located at the cell center, this distribution did not resemble that of the ERC. As shown in KB-CP.5 cells, the distribution of Alexa 546-transferrin shows no overlap with that of NBD-sphingomyelin (compare Fig. 3*C* and *D*). In fact, the distribution of NBD-sphingomyelin is very similar to that obtained when these cells were directly labeled with NBD-ceramide (data not shown).

Lipsky and Pagano (25, 26) have shown that NBD-sphingomyelin can be metabolized to NBD-ceramide, which then localizes in the *trans*-Golgi network. We therefore postulated that this change of distribution of cells labeled with NBD-sphingomyelin in the KB-CP.5 cells was due to a very fast metabolism of NBD-sphingomyelin such that NBD-sphingomyelin in the ERC was rapidly being converted to NBD-ceramide, which was what we observed to accumulate at the cell center, inside the *trans*-Golgi network. To test this hypothesis, we labeled cells with NBD-sphingomyelin, chased for 30 minutes, and back exchanged excess plasma membrane NBD-sphingomyelin in a manner identical to experiments shown in Fig. 3. We then extracted the whole-cell lipids using organic solvents and ran them out on TLC plates. These plates also contained NBD-sphingomyelin and NBD-ceramide standards for comparison. We quantified the fluorescent bands from the parental KB-3-1 and KB-CP.5 cells (see Fig. 3*G*) and found that the KB-CP.5 cells were indeed metabolizing NBD-sphingomyelin to NBD-ceramide more rapidly (~1.7-fold faster).

Thus, the altered distribution of the ERC also seems to accompany a change in its properties, which leads to a more rapid sphingomyelin metabolism as compared with the parental cells.

The abnormally distributed ERC tubules in KB-CP.5 cells have lower internal pH compared with parental KB-3-1 cells. As shown above, our results indicate that the abnormal distribution of the ERC tubules in the KB-CP.5 cells has functional consequences, both in terms of abnormal metabolism of lipids such as sphingomyelin and in terms of the enhanced sequestration of labeled cisplatin. We next attempted to address the mechanism behind these observations. We reasoned that a change in pH inside the ERC tubules could account for both observations. A lowered intra-ERC pH could change the protonation status of cisplatin, thereby making it more hydrophobic. Similarly, a lowered pH would make acid sphingomyelinases more active, thereby increasing sphingomyelin metabolism and its conversion to ceramide.

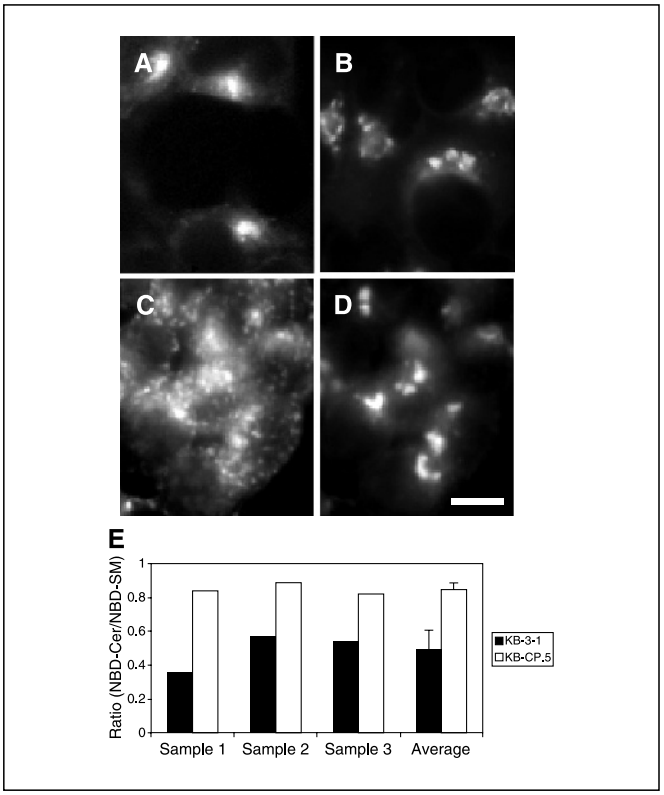

Figure 3. Sphingomyelin trafficking and metabolism measured in KB-3-1 and KB-CP.5 cells. *A* and *B,* NBD-sphingomyelin labeling of KB-3-1 (*A*) and KB-CP.5 (*B*) cells. The cells were labeled with NBD-sphingomyelin at 37° for 1 minute, chased for 30 minutes to achieve steady-state distribution, back exchanged on ice to remove excess cell surface label, and then imaged using wide-field microscopy. Bar, 10 μm. *C* and *D,* KB-CP.5 cells double labeled with Alexa 546-transferrin (*C*) and NBD-sphingomyelin (*D*). Negligible colocalization is observed. Bar, 10 μm. *E,* ratio of NBD-ceramide to NBD-sphingomyelin in KB-3-1 cells (*black columns*) and KB-CP.5 cells (*white columns*) after excess NBD-sphingomyelin on the plasma membrane has been removed by back exchange. The NBD-lipid ratio thus represents primarily the NBD-lipid proportions in the ERC (because most of the NBD-sphingomyelin from the plasma membranes is removed by the back-exchange procedure). The protocol used for the NBD-lipid ratio assay is explained in Materials and Methods. The first three sets of columns in the figure show three independent measurements whereas the fourth set of columns shows the average of these measurements along with the SD.

To test this possibility, we labeled human transferrin simultaneously with both Alexa 546 and fluorescein. The idea was to have both red (Alexa 546) and green (fluorescein) labels on the same transferrin molecule. Fluorescein fluorescence intensity is pH sensitive with the intensity decreasing with the lowering of pH. On the contrary, Alexa 546 fluorescence is pH insensitive. Thus, when cells are labeled with the double-labeled transferrin and the transferrin is allowed to chase into the ERC, its green fluorescence intensity will be indicative of the pH within the compartment, whereas the red fluorescence will provide an internal control of the degree of loading of the particular tubule. We labeled both KB-CP.5 cells and the parental KB-3-1 controls with the double-labeled transferrin and let them reach steady state. We then imaged these cells in both the red and the green channels and determined the

Downloaded from cancerres.aacrjournals.org on May 15, 2021. © 2006 American Association for Cancer Research.

red/green fluorescence intensity ratio (Fig. 4). We found that the ERCs of cisplatin-resistant KB-CP cells exhibited an increased R/F ratio as compared with parental KB cells, indicating thereby that KB-CP cells, on average, have lower pH in the ERC tubules relative to parental controls. This observation points to a possible mechanism by which the KB-CP ERCs are able to sequester cisplatin as well as have increased sphingomyelin metabolism.

The altered distribution of the ERC tubules in cisplatin-resistant cells is dependent on the expression of Glu-α-tubulin. We next addressed the molecular mechanism that might cause the abnormal distribution of the ERC tubules in KB-CP.5 cells. Another cell line that has been extensively studied in our laboratory, and has dispersed the ERC under specialized conditions, is B104-5. Under normal permissive conditions, this cell line behaves identically to its parental cell line, TRVb-1, a CHO cell line that lacks endogenous transferrin receptors and instead expresses transfected human transferrin receptors. The B104-5 cells have a temperature-dependent increase in the level of Glu-α-tubulin (27). The cells were incubated at two different temperatures, 32°C (permissive) and 39°C (nonpermissive), for 3 days before fixation, then permeabilized and immunostained for Glu-α-tubulin. B104-5 cells incubated at 32°C have relatively low levels of stable Glu-α-tubulin, which is found as a network aggregated in linear, polygonal, or irregular-shaped plaques of high fluorescence density near the nuclei of the cells (Fig. 5*A*). An elevated level of Glu-α-tubulin, which appeared loosely arranged and spread throughout the cytoplasm, is detected in the B104-5 cells after 3 days at 39°C, the nonpermissive temperature (Fig. 5*A*). However, the expression level of Tyr-α-tubulin in B104-5 cells grown at 39°C was not significantly different from that in cells incubated at the permissive 32°C (Fig. 5*A*). No alterations in the structural appearance of the Tyr-α-tubulin could be detected and the overall appearance was fairly similar in B104-5 cells cultured at both temperatures. This is consistent with previous results indicating that the elevated expression of Glu-α-tubulin at the restrictive temperature could return to the lower level of Glu-α-tubulin by lowering the temperature of B104-5 cells (18, 27).

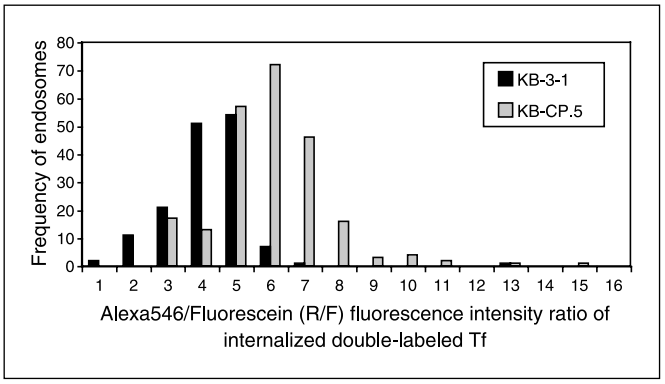

Figure 4. Frequency distribution of the ratios of Alexa 546 to fluorescein (*R/F ratio*) in transferrin-labeled KB-3-1 cells (*black columns*) and KB-CP.5 cells (*gray columns*). The cells were labeled for 30 minutes at 37°C with transferrin double labeled with Alexa 546 (red fluorescence; pH insensitive) and fluorescein (green fluorescence; pH sensitive). They were then rinsed and chased for an additional 10 minutes at 37°C in the presence of deferroxamine (an iron chelator) and 10-fold excess unlabeled transferrin to prevent rebinding of labeled transferrin. The cells were then fixed with 3% paraformaldehyde for 2 minutes at room temperature and imaged using wide-field microscopy. The Alexa 546/fluorescein ratio was measured after background correction. Increasing Alexa 546/fluorescein ratio indicates increasing pH values.

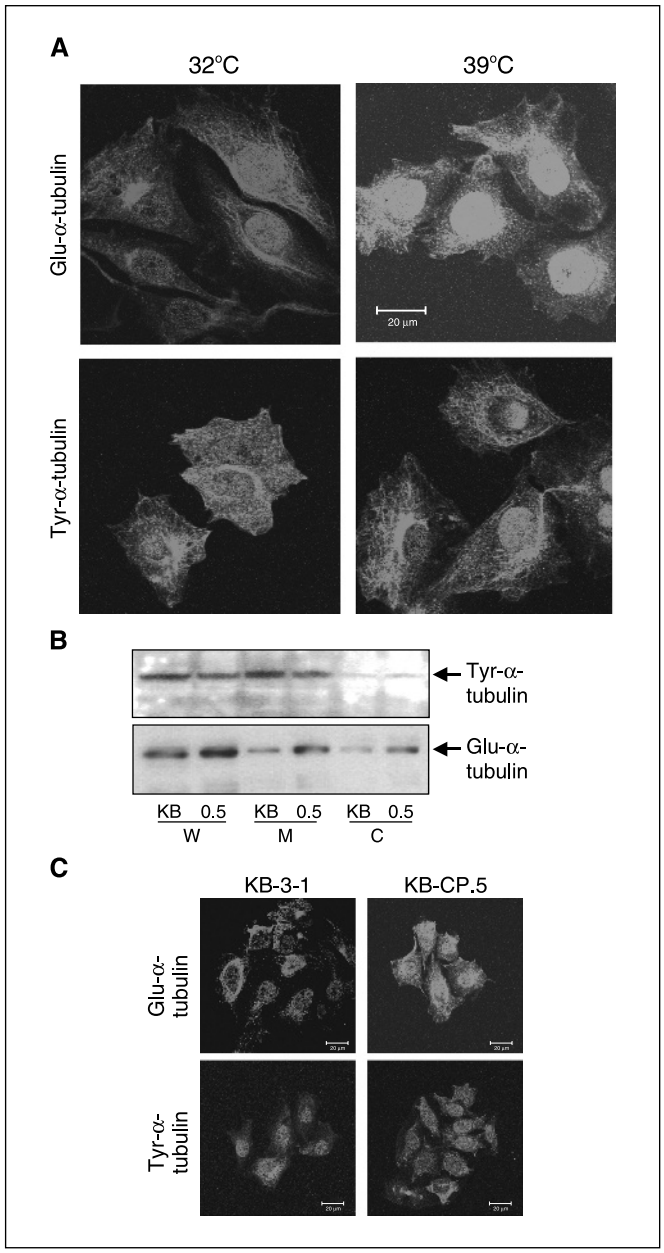

Figure 5. Expression of Glu-α-tubulin and Tyr-α-tubulin by Western blotting and confocal microscopy. *A,* expression of Glu-α-tubulin and Tyr-α-tubulin in B104-5 cells under permissive and nonpermissive conditions. B104-5 cells were incubated under permissive (32°C) and nonpermissive (39°C) conditions for 3 days in 5% CO_2; then cells were fixed and permeabilized as described in Materials and Methods. Several fields of cells were captured and one representative field of each is shown. Bar, 20 μm. *B,* detection of Glu-α-tubulin and Tyr-α-tubulin in isolated fractions of KB-3-1 and KB-CP.5 cells. Fractions (*W,* whole-cell lysis; *M,* plasma membrane enriched fraction; *C,* cytosol fraction) were isolated by different types of ultracentrifugation as described in Materials and Methods. *C,* immunofluorescence pictures of KB-3-1 and KB-CP.5 cells stained with antibodies against Glu-α-tubulin and Tyr-α-tubulin. A pronounced aggregation of Glu-α-tubulin near the nuclei in KB-3-1 cells is observed compared with KB-CP.5 cells. No changes in the cytoplasmic distribution pattern of the Tyr-α-tubulin are detectable. Representative of at least six images.

The distribution of the ERC and Glu-α-tubulin was then examined in KB-3-1 and KB-CP.5 cells. The expression of Glu-α-tubulin was found to be increased in KB-CP.5 cells compared with parental KB-3-1 cells as detected by Western blotting. As shown in Fig. 5*B*, there is a higher level of Glu-α-tubulin expression

Downloaded from cancerres.aacrjournals.org on May 15, 2021. © 2006 American Association for Cancer Research.

in KB-CP.5 cells compared with parental KB-3-1 cells. We did not detect any major difference in the expression of Tyr-α-tubulin between the cisplatin-resistant KB-CP.5 and cisplatin-sensitive KB-3-1 cells. Based on immunohistochemistry, parental KB-3-1 cells have a relatively clustered distribution of down-regulated, stable Glu-α-tubulin near the nuclei of the cells. An elevated level of Glu-α-tubulin was also detected in the cisplatin-resistant KB-CP.5 cells but with a dispersed distribution of Glu-α-tubulin throughout the cytoplasm (Fig. 5*C*). However, there was no significant alteration in the appearance or expression level of Tyr-α-tubulin in the resistant KB-CP.5 cells (Fig. 5*C*), which was similar to the results with B104-5 cells mentioned above. The results indicate that there is a correlation between the levels of stable Glu-α-tubulin and the appearance of the ERC and suggest that stable microtubules containing elevated levels of Glu-α-tubulin might play a role in vesicle recycling or transportation.

B104-5 cells are relatively resistant to cisplatin under nonpermissive conditions. To determine whether the formation of an irregular ERC might lead to cisplatin resistance, we compared the cisplatin toxicity of B104-5 cells at permissive and nonpermissive temperatures. B104-5 cells were incubated with various cisplatin concentrations at 32°C (permissive) or 39°C (nonpermissive) for 4 weeks. Based on a colony-forming assay, there was a 2.0-fold difference in cisplatin resistance between the B104-5 cells at the nonpermissive temperature (0.31 μg/mL) and B104-5 cells incubated at the permissive temperature (0.15 μg/mL; Fig. 6*A*). Similar results were found using a 72-hour cell proliferation assay with ~4-fold resistance to cisplatin at the nonpermissive temperature. However, there was no significant difference in cisplatin resistance between the TRVb-1 CHO parental cells at the permissive temperature (32°C) and nonpermissive temperature (39°C; Fig. 6*B*). Therefore, temperature-sensitive B104-5 cells with overexpressed Glu-α-tubulin were more resistant to cisplatin at the nonpermissive temperature compared with parental TRVb-1 CHO cells.

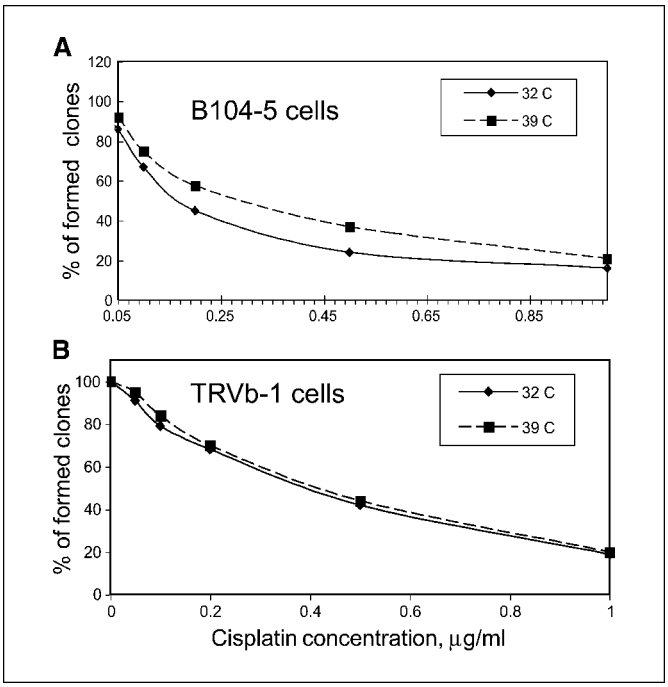

Figure 6. Cytotoxicity of cisplatin measured in cells with different ERC structures. *A,* the cytotoxicity of cisplatin in B104-5 cells incubated at permissive or nonpermissive temperature was determined by colony-forming assays 4 weeks after continuous exposure to cisplatin at different concentrations. The results are expressed as the percent of viable cisplatin-treated cells compared with untreated cells. *Points,* mean of triplicate measurements; *bars,* SE. *B,* colony-forming assay to measure the cisplatin resistance of parental TRVb-1 CHO cells. After the cells were incubated in medium with various concentrations of cisplatin, cells were treated and counted as described in Materials and Methods.

Discussion

Cellular resistance to cisplatin is multifactorial and may consist of mechanisms limiting the formation of DNA adducts, repair mechanisms and alterations that promote cell survival (28, 29). The formation of DNA adducts by cisplatin can be limited by reduced drug accumulation, enhanced drug efflux, sequestration of drugs within the cytoplasm, and inactivation of platinum drugs by coordination of sulfur-containing compounds (30). Details of the mechanisms underlying the antitumor activity of cisplatin or resistance to this drug are not entirely understood despite intensive research in this area (31). However, reduced accumulation of cisplatin seems to be a common mechanism of resistance (32). In this work, we monitored the trafficking of the bona fide ERC marker, transferrin, bound to its receptor, as well as several fluorescent membrane lipid analogues, through the ERC. Our previous study and the work of others have shown that altered uptake of cisplatin occurs because of reduced membrane-binding/transport proteins and reduced endocytosis (2, 33). Here, we show that there is a defect in the localization and probably the function of the ERC, consistent with a shown alteration in the level of Glu-α-tubulin (in stable, detyrosinated microtubules).

In most cell types, ~95% of endocytosed membrane is recycled to the plasma membrane. This recycling is important for the maintenance of membrane composition and for cell-surface expression of receptors involved in nutrient uptake as well as for several other cellular processes (34, 35). We used fluorescently labeled transferrin to study the lipid recycling pathway and found that the ERC is altered in KB-CP.5 cells compared with KB-3-1 cells. This was confirmed by other known ERC markers. A tightly clustered ERC is located near the nucleus in parental KB-3-1 cells but it appears loosely arranged and widely dispersed throughout the cytoplasm in KB-CP.5 cells. The overall distribution of the ERC in these cells is related to the amount and distribution of stable detyrosinated microtubules. The structural and functional integrity of the ERC in part depends on the cytoskeleton, which seems to be involved in regulating molecular sorting and vesicular transport of the ERC with microtubules (36). In this work, we found that B104-5 cells sensitive to temperature are more resistant to cisplatin, with an altered ERC due to stable Glu-α-tubulin–containing microtubules, at nonpermissive temperature than at permissive temperature.

There are only a few hints to a possible influence of the cytoskeleton on cisplatin resistance. Cisplatin can affect cytoplasmic actin filaments as seen in qualitative histologic and ultrastructural findings (37). Biochemical studies done with isolated tubulin molecules showed that cisplatin was able to inhibit irreversibly the polymerization of microtubules by covalent binding to sulfhydryl groups in tubulin dimers (38). Most mammalian cells possess two subsets of microtubules: dynamic microtubules with a half-life of 5 to 10 minutes and stable microtubules with a half-life of hours (39). Dynamic microtubules

Downloaded from cancerres.aacrjournals.org on May 15, 2021. © 2006 American Association for Cancer Research.

contain mainly tyrosinated tubulin (Tyr-α-tubulin). Stable microtubules contain various modified tubulins, including detyrosinated tubulin (Glu-α-tubulin), which accumulate in stable microtubules but do not cause microtubule stabilization (40). The best-characterized modification of tubulin is detyrosination, which involves the reversible removal of the COOH-terminal Tyr residue from α-tubulin, exposing a Glu residue as the new COOH terminus (41, 42). Stable microtubules are important in the distribution of the ERC (27).

We chose B104-5 cells to study the effects of the distribution and expression pattern of tubulin on cisplatin resistance. B104-5 has a striking temperature-induced alteration of Glu-α-tubulin associated with the morphology of its ERC. Under permissive conditions, a tightly clustered ERC is located near the Golgi complex in B104-5 cells cultured at 32°C. Under nonpermissive conditions at 39°C, this compartment appears fragmented and widely dispersed. Surprisingly, this alteration in the morphology of the recycling compartment has no effect on the kinetics of receptor internalization and recycling (18). The wild-type endocytic compartment is closely aligned with the microtubule-organizing center and the Golgi apparatus, and like the Golgi, its clustered appearance is dependent on intact microtubules. Lin et al. (27) found that treatment with taxol could increase expression of stable Glu-α-tubulin in the B104-5 cells, which resulted in a dispersed ERC structure similar to when cells were incubated at 39°C. In this work, we show that B104-5 cells with a dispersed ERC incubated under nonpermissive temperature were more resistant to cisplatin compared with B104-5 cells with a more clustered ERC structure under incubation at permissive temperature. It is very possible that resistance to cisplatin is due to the formation of the ERC, which accumulates active cisplatin inside its vesicles, reduces trafficking of cisplatin from the cell surface into the cell, and limits the possibility of cisplatin forming DNA adducts in the nucleus.

It should, however, be noted that B104-5 cells have been previously shown to overexpress certain heat shock proteins (see discussion in ref. 18). It is thus possible that increased cisplatin resistance of B104-5 cells under nonpermissive conditions is more related to a general up-regulation of heat shock type response than to a direct effect of the altered ERC. Could the increased cisplatin-resistant of KB-CP.5 cells also be due to some other phenomenon which may be upstream from the ERC defect? Although this is a possibility, the finding of cisplatin and methotrexate colocalized with the altered ERC structures argues in favor of a direct effect of the altered ERC on cisplatin resistance.

It is well established that organelles along both the secretory and endocytic pathways experience a gradient of decreasing pH (13). We found that the pH of the ERC is more acidic in cisplatin-resistant KB-CP.5 cells compared with parental KB-3-1 cells. This was determined by directly measuring the pH of late endosomes/lysosomes by ratio fluorescence imaging. Acidification of endosomes is necessary for a variety of essential eukaryotic cellular functions (13). However, the mechanisms that regulate pH in these organelles are complex and not yet completely understood. In general, endosomal acidity is generated by the membrane-bound ATP-dependent proton pump (vacuolar H^+-ATPase) and the degree of acidification is modulated by a complex interplay of this pump and several other pumps or transporters, including the Na^+-K^+-ATPase and chloride channels (13). Further investigation will be required to pinpoint precisely which of these protein(s) is/are affected in the KB-cisplatin–resistant cells.

pH changes in the ERC in the cisplatin-resistant cells might cause cisplatin to be "trapped" in the ERC due to the low permeability of the charged cisplatin to vesicular membranes, which would diminish the toxicity of cisplatin in KB-CP.5 cells. In addition, the normal distribution of the ERC and intracellular trafficking through this organelle could be disrupted by an acidic alteration. It is therefore possible that cisplatin-resistant cells could sequester cisplatin in an acidic ERC and expel it from the cells by exocytosis. However, in previous work, we found alkalinization of lysosomes in cisplatin-resistant cells (23). Why the pH differs in lysosomes and the ERC in cisplatin-resistant cells is still unclear. These pH changes in the endocytic pathway need further study. In addition, we have found in this study that NBD-sphingomyelin, of which the bulk of intracellular pool localizes to the ERC at steady state, is metabolized significantly faster into NBD-ceramide in cisplatin-resistant KB-CP.5 cells. It will be interesting to explore whether this acceleration of sphingomyelin metabolism is correlated with increased activation of acid sphingomyelinases in the ERC of cisplatin-resistant cells due to a lowering of the pH. Because ceramide is a known second messenger, we speculate that such increased production of ceramide in the ERC might play a role in the carcinogenesis process.

The dispersed ERC localization and the elevated expression of Glu-α-tubulin in KB-CP.5 cells permit a better examination of the association of the ERC with cisplatin resistance in B104-5 cells. Reports of platinum-rich phagocytic granules (platinosomes), which may be related to lysosomes or the ERC, suggested that cisplatin might localize in these intracellular lysosome-like organelles. In addition, relatively high concentrations of cisplatin were found in microsomal fractions of liver and kidney tissues following cisplatin administration (43). Using confocal microscopy, we found nearly all of the internalized Alexa 488-cisplatin in the ERC labeled with Texas red-transferrin in KB-CP.5 cells, similar to internalized Alexa 546–labeled methotrexate (Fig. 4). Therefore, it is probable that alterations in the cytoskeleton related to Glu-α-tubulin are sufficient to alter the spatial distribution of intracellular cisplatin. It is worth mentioning that, following treatment with cisplatin, the number of platinum atoms bound covalently to cytoplasmic proteins quantitatively exceeds the number of platination sites on the nuclear DNA (44). These results suggest that nuclear DNA is not the only target of the intracellular action of cisplatin and reveal that additional molecular lesions must occur independently of the molecular attachment to DNA, which could result, for example, in structural alterations to the ERC. As mentioned earlier, we have found that NBD-C6-sphingomyelin was metabolized faster into NBD-C6-ceramide in cisplatin-resistant KB-CP.5 cells. Therefore, altered phospholipid metabolism or trafficking in tumor cells that are cisplatin-resistant may represent a novel target for new anticancer agents.

Acknowledgments

Received 9/27/2005; revised 11/23/2005; accepted 12/12/2005.

Grant support: This research was supported, in part, by the Intramural Research Program of the NIH, Center for Cancer Research, National Cancer Institute, and NIH grant DK27083 (F. Maxfield and S. Mukherjee).

The costs of publication of this article were defrayed in part by the payment of page charges. This article must therefore be hereby marked *advertisement* in accordance with 18 U.S.C. Section 1734 solely to indicate this fact.

We thank George Leiman for his assistance with editing of this manuscript and Drs. Susan H. Garfield and Stephen M. Wincovitch for their technical assistance with confocal microscopy.

Downloaded from cancerres.aacrjournals.org on May 15, 2021. © 2006 American Association for Cancer Research.

References

1. Wang G, Reed E, Li QQ. Molecular basis of cellular response to cisplatin chemotherapy in non-small cell lung cancer. Oncol Rep 2004;12:955–65.
2. Safaei R, Howell SB. Copper transporters regulate the cellular pharmacology and sensitivity to Pt drugs. Crit Rev Oncol Hematol 2005;53:13–23.
3. Shen DW, Su A, Liang XJ, Pai-Panandiker A, Gottesman MM. Reduced expression of small GTPases and hypermethylation of the folate binding protein gene in cisplatin-resistant cells. Br J Cancer 2004;91:270–6.
4. Pinto AL, Lippard SJ. Binding of the antitumor drug *cis*-diamminedichloroplatinum(II) (cisplatin) to DNA. Biochim Biophys Acta 1985;780:167–80.
5. Chu G. Cellular response to cisplatin: The roles of DNA binding proteins and DNA repair. J Biol Chem 1994;269:787–90.
6. Siddik ZH. Biochemical and molecular mechanisms of cisplatin resistance. Cancer Treat Res 2002;112:263–84.
7. Speelmans G, Sips WH, Grisel RJ, et al. The interaction of the anti-cancer drug cisplatin with phospholipids is specific for negatively charged phospholipids and takes place at low chloride ion concentration. Biochim Biophys Acta 1996;1283:60–6.
8. Speelmans G, Staffhorst RW, Versluis K, Reedijk J, de Kruijff B. Cisplatin complexes with phosphatidylserine in membranes. Biochemistry 1997;36:10545–50.
9. Burger KN, Staffhorst RW, De Kruijff B. Interaction of the anti-cancer drug cisplatin with phosphatidylserine in intact and semi-intact cells. Biochim Biophys Acta 1999;1419:43–54.
10. Liang XJ, Yin JJ, Zhou JW, et al. Changes in biophysical parameters of plasma membranes influence cisplatin resistance of sensitive and resistant epidermal carcinoma cells. Exp Cell Res 2004;293:283–91.
11. Maheswari KU, Ramachandran T, Rajaji D. Interaction of cisplatin with planar model membranes does dependent change in electrical characteristics. Biochim Biophys Acta 2000;1463:230–40.
12. Liang XJ, Shen DW, Garfield S, Gottesman MM. Mislocalization of membrane proteins associated with multidrug resistance in cisplatin-resistant cancer cell lines. Cancer Res 2003;63:5909–16.
13. Mukherjee S, Ghosh RN, Maxfield FR. Endocytosis. Physiol Rev 1997;77:759–803.
14. Maxfield FR, McGraw TE. Endocytic recycling. Nat Rev Mol Cell Biol 2004;5:121–32.
15. Nichols BJ, Kenworthy AK, Polishchuk RS, et al. Rapid cycling of lipid raft markers between the cell surface and Golgi complex. J Cell Biol 2001;153:529–41.
16. Hopkins CR, Trowbridge IS. Internalization and processing of transferrin and the transferrin receptor in human carcinoma A431 cells. J Cell Biol 1983;97:508–21.
17. Akiyama S, Fojo A, Hanover JA, Pastan I, Gottesman MM. Isolation and genetic characterization of human KB cell lines resistant to multiple drugs. Somat Cell Mol Genet 1985;11:117–26.
18. McGraw TE, Dunn KW, Maxfield FR. Isolation of a temperature-sensitive variant Chinese hamster ovary cell line with a morphologically altered endocytic recycling compartment. J Cell Physiol 1993;155:579–94.
19. Mukherjee S, Soe TT, Maxfield FR. Endocytic sorting of lipid analogues differing solely in the chemistry of their hydrophobic tails. J Cell Biol 1999;144:71–1284.
20. Koval M, Pagano RE. Lipid recycling between the plasma membrane and intracellular compartments: transport and metabolism of fluorescent sphingomyelin analogues in cultured fibroblasts. J Cell Biol 1989;108:2169–81.
21. Mayor S, Presley JF, Maxfield FR. Sorting of membrane components from endosomes and subsequent recycling to the cell surface occurs by a bulk flow process. J Cell Biol 1993;12:1257–69.
22. Pagano RE, Watanabe R, Wheatley C, Dominguez M. Applications of BODIPY-sphingolipid analogs to study lipid traffic and metabolism in cells. Methods Enzymol 2000;312:523–34.
23. Chauhan SS, Liang XJ, Su AW, et al. Reduced endocytosis and altered lysosome function in cisplatin-resistant cell lines. Br J Cancer 2003;88:1327–34.
24. Liang XJ, Shen DW, Chen KG, Wincovitch SM, Garfield SH, Gottesman MM. Trafficking and localization of platinum complexes in cisplatin-resistant cell lines monitored by fluorescence-labeled platinum. J Cell Physiol 2005;202:635–41.
25. Lipsky NG, Pagano RE. Sphingolipid metabolism in cultured fibroblasts: microscopic and biochemical studies employing a fluorescent ceramide analogue. Proc Natl Acad Sci U S A 1983;80:2608–12.
26. Lipsky NG, Pagano RE. Intracellular translocation of fluorescent sphingolipids in cultured fibroblasts: endogenously synthesized sphingomyelin and glucocerebroside analogues pass through the Golgi apparatus en route to the plasma membrane. J Cell Biol 1985;100:27–34.
27. Lin SX, Gundersen GG, Maxfield FR. Export from pericentriolar endocytic recycling compartment to cell surface depends on stable, detyrosinated (glu) microtubules and kinesin. Mol Biol Cell 2002;13:96–109.
28. Andrews PA, Howell SB. Cellular pharmacology of cisplatin: perspectives on mechanisms of acquired resistance. Cancer Cell 1990;2:35–43.
29. Stein WD, Litman T, Fojo T, Bates SE. Differential expression of cell adhesion genes: Implications for drug resistance. Int J Cancer 2005;113:861–5.
30. Brabec V, Kasparkova J. Molecular aspects of resistance to antitumor platinum drugs. Drug Resist Updat 2002;5:147–61.
31. Agarwal R, Kaye SB. Ovarian cancer: strategies for overcoming resistance to chemotherapy. Nat Rev Cancer 2003;3:502–16.
32. Shen DW, Goldenberg S, Pastan I, Gottesman MM. Decreased accumulation of [^{14}C]carboplatin in human cisplatin-resistant cells results from reduced energy-dependent uptake. J Cell Physiol 2000;183:108–16.
33. Gruenberg J. Lipids in endocytic membrane transport and sorting. Curr Opin Cell Biol 2003;15:382–8.
34. Liang XJ, Shen DW, Gottesman MM. A pleiotropic defect reducing drug accumulation in cisplatin-resistant cells. J Inorg Biochem 2004;98:1599–606.
35. Gruenberg J, Stenmark H. The biogenesis of multivesicular endosomes. Nat Rev Mol Cell Biol 2004;5:317–23.
36. Coumailleau F, Das V, Alcover A, et al. Overexpression of Rififylin, a new RING finger and FYVE-like domain-containing protein, inhibits recycling from the endocytic recycling compartment. Mol Biol Cell 2004;15:4444–56.
37. Shen DW, Liang XJ, Gawinowicz MA, Gottesman MM. Identification of cytoskeletal [^{14}C]carboplatin-binding proteins reveals reduced expression and disorganization of actin and filamin in cisplatin-resistant cell lines. Mol Pharmacol 2004;66:789–93.
38. Tulub AA, Stefanov VE. Cisplatin stops tubulin assembly into microtubules. A new insight into the mechanism of antitumor activity of platinum complexes. Int J Biol Macromol 2001;28:191–8.
39. Palazzo A, Ackerman B, Gundersen GG. Cell biology: Tubulin acetylation and cell motility. Nature 2003;421:230.
40. Webster DR, Wehland J, Weber K, Borisy GG. Detyrosination of α-tubulin does not stabilize microtubules *in vivo*. J Cell Biol 1990;111:113–22.
41. Wehland J, Weber K. Turnover of the carboxy-terminal tyrosine of α-tubulin and means of reaching elevated levels of detyrosination in living cells. J Cell Sci 1987;88:185–203.
42. Gundersen GG, Kalnoski MH, Bulinski JC. Distinct populations of microtubules: tyrosinated and nontyrosinated α-tubulin are distributed differently *in vivo*. Cell 1984;38:779–89.
43. Aggarwal SK, Whitehouse MW, Ramachandran C. Ultrastructural effects of cisplatin. In: Prestayko AW, Crooke ST, Carter SK, editors. Cisplatin: Current Status and New Development. New York: Academic Press; 1980.
44. Kopf-maier P, Huhlhausen SK. Changes in the cytoskeleton pattern of tumor cells by cisplatin *in vitro*. Chem Biol Interact 1992;82:295–316.

Downloaded from cancerres.aacrjournals.org on May 15, 2021. © 2006 American Association for Cancer Research.

AACR American Association for Cancer Research

Cancer Research
The Journal of Cancer Research (1916–1930) | The American Journal of Cancer (1931–1940)

Endocytic Recycling Compartments Altered in Cisplatin-Resistant Cancer Cells

Xing-Jie Liang, Sushmita Mukherjee, Ding-Wu Shen, et al.

Cancer Res 2006;66:2346-2353.

Updated version	Access the most recent version of this article at: http://cancerres.aacrjournals.org/content/66/4/2346

Cited articles	This article cites 41 articles, 13 of which you can access for free at: http://cancerres.aacrjournals.org/content/66/4/2346.full#ref-list-1
Citing articles	This article has been cited by 10 HighWire-hosted articles. Access the articles at: http://cancerres.aacrjournals.org/content/66/4/2346.full#related-urls

E-mail alerts	Sign up to receive free email-alerts related to this article or journal.
Reprints and Subscriptions	To order reprints of this article or to subscribe to the journal, contact the AACR Publications Department at pubs@aacr.org.
Permissions	To request permission to re-use all or part of this article, use this link http://cancerres.aacrjournals.org/content/66/4/2346. Click on "Request Permissions" which will take you to the Copyright Clearance Center's (CCC) Rightslink site.

Downloaded from cancerres.aacrjournals.org on May 15, 2021. © 2006 American Association for Cancer Research.